Bioorganic Chemistry 58 (2015) 65–71

Contents lists available at ScienceDirect

Bioorganic Chemistry

journal homepage: www.elsevier.com/locate/bioorg

Organocatalyzed solvent free an efficient novel synthesis of 2,4,5-trisubstituted imidazoles for α-glucosidase inhibition to treat diabetes

Muhammad Yar [a,*], Marek Bajda [b,c], Sohail Shahzad [a,d], Nisar Ullah [e], Mazhar Amjad Gilani [f], Muhammad Ashraf [g], Abdul Rauf [d], Ayesha Shaukat [g]

[a] Interdisciplinary Research Center in Biomedical Materials, COMSATS Institute of Information Technology, Lahore 54000, Pakistan
[b] Faculty of Chemistry, University of Warsaw, Pasteura 1, 02-093 Warsaw, Poland
[c] Department of Physicochemical Drug Analysis, Faculty of Pharmacy, Jagiellonian University Medical College, Medyczna 9, 30-688 Cracow, Poland
[d] Department of Chemistry, The Islamia University of Bahawalpur, Bahawalpur 63100, Pakistan
[e] Department of Chemistry, King Fahd University of Petroleum and Minerals, Dhahran 31261, Saudi Arabia
[f] Department of Chemical Engineering, COMSATS Institute of Information Technology, Lahore 54000, Pakistan
[g] Department of Biochemistry & Biotechnology, The Islamia University of Bahawalpur, Bahawalpur 63100, Pakistan

ARTICLE INFO

Article history:
Received 9 August 2014
Available online 21 November 2014

Keywords:
Imidazoles
α-glucosidase inhibition
Diabetes
Organocatalysis
Molecular modeling
Baker's yeast

ABSTRACT

A new and efficient solvent free synthesis of 2,4,5-trisubstituted imidazoles (**3a**–**3j**) was achieved by N-acetyl glycine (NAG) catalyzed three components condensation of aldehydes, benzil and ammonium acetate. Our synthetic methodology accommodated a range of various substituted alkyl and aryl aldehydes. Evaluation of α-glucosidase inhibitory activity of these imidazole derivatives revealed that most of them presented good α-glucosidase inhibition at low micro-molar concentrations. Among the synthesized compounds, compound **3c**, bearing the *ortho*-hydroxy phenyl substituent at position 2 displayed the highest inhibitory activity with an IC_{50} value 74.32 ± 0.59 μM. *In silico* molecular docking for all compounds and computational studies of the most active compound **3c** were also performed.

1. Introduction

Diabetes mellitus is a group of metabolic disorders which result from defects in both regulations of insulin secretion and/or insulin action. As a result, the glucose concentration in the blood increases (hyperglycemia) and over time causes serious damage to many of the body's organs, especially the nerves and blood vessels [1]. Since 1980, the number of people in the world with diabetes has increased from 153 million to 347 million in 2008 [2]. Based on the WHO projection, diabetes will become seventh leading cause of death globally by 2030. One therapeutic approach for diabetes is to control the postprandial glucose levels and suppress postprandial hyperglycemia by inhibition of carbohydrate-hydrolyzing enzymes, such as α-glucosidase [3,4]. α-Glucosidase inhibitors reversibly inhibit digestive α-glucosidase, which retard the liberation of glucose from dietary complex carbohydrate and starch, delaying absorption of glucose into the bloodstream and, thus reducing plasma glucose levels. Inhibition of α-glucosidase has drawn a special interest by the pharmaceutical research community as a remedy for the treatment of carbohydrate mediated diseases such as cancer, viral infections, diabetics and hepatitis [5–7]. The inhibitors of α-glucosidase are known to possess antitumor, antidiabetics, antiviral, and immunoregulatory activities [8–10]. In addition, α-glucosidase inhibitors such as deoxynojirimycin (DNJ), N-butyl-deoxynojirimycin (NB-DNJ) and castanospermine are potent inhibitors of the HIV replication and HIV mediated syncytium formation *in vitro* [10].

Currently, glucosidic based α-glucosidase inhibitors such as acrabose [11], miglitol [12], voglibose [13] and nojirimycin [14] are clinically used to control blood glucose levels of patients (Fig. 1). Although effective, these inhibitors suffer from liabilities such as abdominal distension, flatulence, meteorism and possibly diarrhea [15]. In order to search for more effective and safer α-glucosidase inhibitors, efforts have been devoted in the development of non-glucosidic based inhibitors [16,17].

Substituted imidazoles are known to possess a range of therapeutic effects such as potent and selective inhibitors of p38 MAP kinase [18], B-Raf kinase [19], transforming growth factor b1 (TGF-b1) type 1 activating receptor-like kinase (ALK5) [20],

* Corresponding author. Fax: +92 42 35321090.
E-mail address: drmyar@ciitlahore.edu.pk (M. Yar).

http://dx.doi.org/10.1016/j.bioorg.2014.11.006
0045-2068/

cyclooxygenase-2 (COX-2) [21], and biosynthesis of interleukin-1 (IL-1) [22]. In addition, SB-220109 (Fig. 2) is reported as potent p38α recaptulates protein kinase inhibitor [23].

Generally 2,4,5-trisubstituted imidazoles are synthesized by three component cyclocondensation of a 1,2-diketone, α-hydroxyketone or α-ketomonoxime with an aldehyde and ammonium acetate using a variety of different catalysts including L-proline [24], montmorillonite K10 [25], zeolite [25], nano sulfated zirconia [25], 1-ethyl-3-methylimidazole acetate [EMIM]OAc [26], zirconium (IV) acetylacetonate ($Zr(acac)_4$) [27], 1-(2-hydroxyethyl)-3-methyl imidazoliumtetrafluoroborate ($[HeMIM]BF_4$) [28], acetic acid (HOAc) [29], tetrabutylammonium bromide (TBAB) [30], polymer supported zinc chloride [31], supported ionic liquid like phase (SILLP) [32], Nano-$SnCl_4$. SiO_2 [33], L-cysteine [34], 1-methylimidazolium trifluoroacetate ([Hmim]TFA) [35] and potassium dihydrogen phosphate [36].

Most of these synthetic methods suffer from one or more serious limitations including laborious and complex work-up and purification, significant amounts of waste materials, strongly acidic conditions, occurrence of side reactions, low yields, use of expensive reagents and require elevated temperatures. To overcome these shortcomings, the development of a new organocatalytic system to meet the criteria of a mild, efficient, and environmentally benign protocol for the synthesis of substituted imidazoles is highly desirable. Recently, we have found and reported the use of N-acetyl glycine (NAG) as an efficient organocatalyst in the synthesis of pyrimidines, where the required pyrimidines were achieved in significant to good yields. An easy method was established for the removal of NAG from the reaction mixture after the reaction and the subsequent purification of the targeted pyridmides was straight forward as well [37]. In continuation of our ongoing medicinal chemistry research endeavours [38–41] herein, we disclose a novel and facile NAG organocatalyzed synthesis of 2,4,5-trisubstituted imidazoles under mild and solvent free reaction conditions. The advantages of using N-acetyl glycine (NAG) as an efficient organocatalyst in the synthesis of 2,4,5-trisubstituted imidazoles were included the easy-work up and purification, one pot and one step, avoidance from any acidic conditions, better yields, solvent-free and thus environmentally friendly. *In vitro* α-glucosidase inhibitory activity and *in silico* molecular docking studies of all compounds are also included to demonstrate the binding pattern with the active site of the targeted protein.

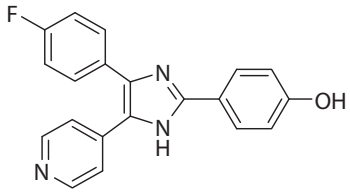

Fig. 2. The molecular structure of SB-220109.

2. Results and discussion

2.1. Chemistry

The desired 2,4,5-trisubstituted imidazoles **3a**–**3j** [25,32–35,42] bearing different substituents were prepared in good to excellent yields (67–85%) as shown in Scheme 1. The preparation of **3a**–**3j** was ensued from condensation of benzil, ammonium acetate and the corresponding aldehydes **2a**–**2j**, catalyzed by NAG. Notably, a variety of functional groups such as hydroxyl, methoxy and chloro were tolerated under our new reaction protocol. The chemical structures of all the synthesized compounds were established with the aid of spectroscopic and physical methods.

2.2. α-Glucosidase inhibition assay

A recurring aspect in enzyme catalyzed reaction mechanisms is the use of proton-transfer processes to affect catalysis. The classic example of this phenomenon is the serine proteases [44], for instance chymotrypsin, where the nucleophilicity of the active-site serine hydroxyl group is enhanced by a histidine-side-chain imidazole nucleus mediated indirect co-ordination to an anionic aspartate residue, in the so-called 'catalytic triad'. The well-characterized general acid-base catalysis employed by glucosidases to ensue cleavage of the glycosidic linkage (for reviews of this topic, see [45] and [46] and references cited therein) led us to speculate that placement of an imidazole unit between the 'acid' and 'base' residues would result in shuttling of a proton between the two groups 'through' the imidazole nucleus. The proposed mechanism of the interaction of the imidazole with the active site of the β-glucosidase enzyme has been elaborated in Scheme 2 [47]. Similar interactions could also be expected among other glucosidases

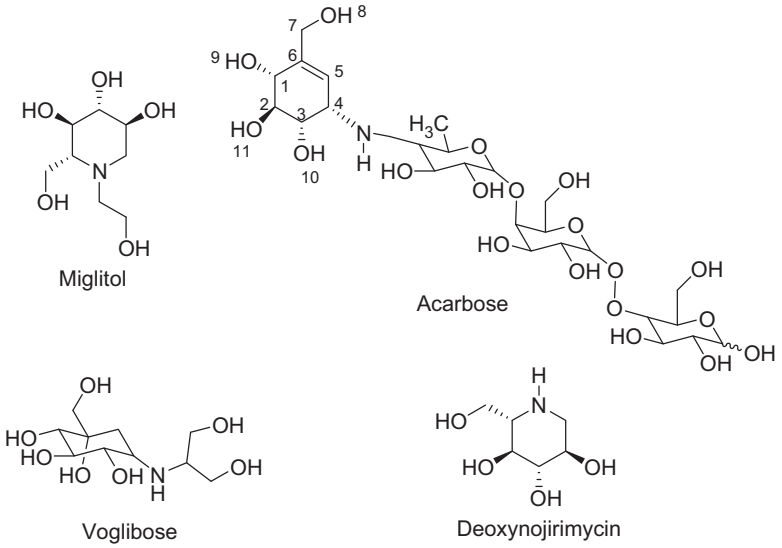

Fig. 1. The α-glucosidase inhibitors: acarbose, voglibose, deoxynojirimycin and miglitol.

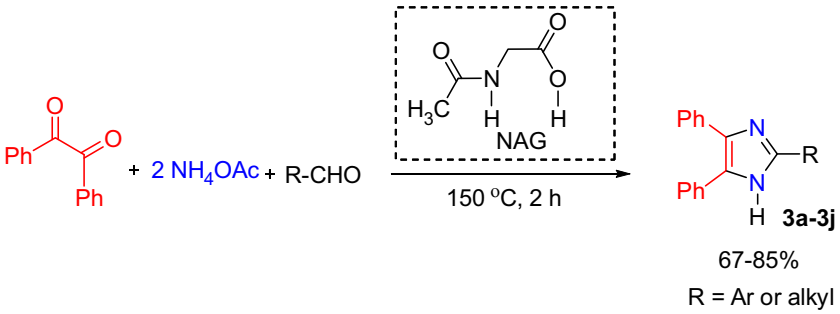

Scheme 1. Synthetic protocol for the NAG catalyzed synthesis of 2,4,5-trisubstituted imidazoles.

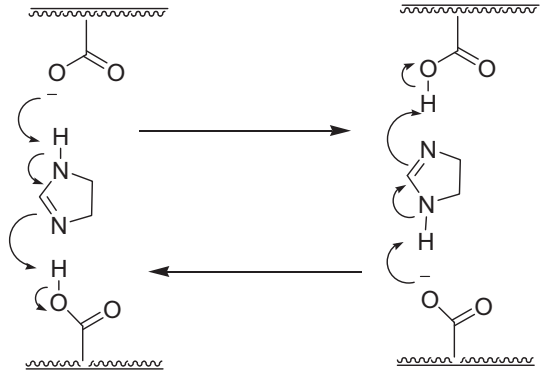

Scheme 2. Mode of interaction of imidazole with active-site catalytic residues of glucosidase enzyme.

and potential acid catalysts such as histidine, tyrosine or Mg^{+2} [45]. Compounds that would bind with glucosidases in the aforementioned manner is expected to be potential inhibitors of such enzymes [48]. Balba et al., determined the *in vivo* and *in vitro* α-glucosidase inhibition activities of 4,5-diphenylimidazole-2-thione. It was described that 4,5-diphenylimidazole-2-thione demonstrated *in vitro* α-glucosidase inhibition by non-competitive reversible mechanism [43].

In the current studies, all the synthesized imidazole derivatives (**3a**–**3j**) were evaluated for α-glucosidase inhibitory activity which revealed that compounds **3c**, **3f** and **3g** were found to be active, showing α-glucosidase inhibition from 96.63 ± 1.11% to 97.63 ± 1.29% at 0.5 mM with IC_{50} values ranged between 106.57 ± 0.86 and 74.32 ± 0.52 μM (Table 1). Acarbose was used as a standard inhibitor.

2.3. Structure activity relationship

In order to delineate the structure–activity relationship and to get an optimized α-glucosidase inhibitor, both benzaldehyde and substituted benzaldehydes as well as alkyl aldehydes were used in the synthesis of these substituted imidazole derivatives (**3a**–**3j**). These substituents include electron donating groups such as hydroxly, methoxy and electron withdrawing group such as chloro substituent. Compound **3c**, bearing 2-hydroxyphenyl moiety at the 2-position of the imidazole ring, was proved to be the most active one with an IC_{50} value of 74.32 ± 0.52 μM. Changing the position of the hydroxyl group in the phenyl ring from C-2 to C-4, producing **3f** (97.12 ± 0.71 μM) slightly diminished the activity. From the activity pattern it can be ascertain that the presence of the hydroxy group in the phenyl ring plays a significant role in the higher activity of these compounds and the activity is higher when hydroxyl group is present at C-2 of the phenyl ring (compounds **3c** vs. **3f**). Likewise compound **3g** (106.57 ± 0.86 μM) possessing hydroxyl group in the phenyl ring at C-2 was also reasonably active compared to the rest of the compounds in the series that do not contain hydroxyl group in the phenyl ring (Table 1). Compound **3a**, bearing unsubstituted phenyl ring was turned out to be inactive and when a chlorine atom was introduced at the C-4 position of the 2-phenyl ring, the resulting derivative **3b** (458.32 ± 1.14 μM) showed modest activity. Similarly, compound **3d** (359.42 ± 1.12 μM), possessing a methoxy group at C-3 turned out to be modestly active compared to its parent compound **3a** (Table 1).

2.4. Molecular modeling

The novel compounds **3a**–**3j** were tested in α-glucosidase assay and displayed different activities. The most active inhibitor **3c** *ortho*-hydroxy analogue of **3a** was 2-fold less potent than reference compound – acarbose while the parent compound **3a** was almost inactive. Therefore, we decided to perform docking studies to find the possible binding mode for all derivatives and to explain the reasons of the varied potency.

As α-glucosidase from baker's yeast was utilized in biological experiments, we needed to use the enzyme from the same source for *in silico* modeling. The crystal structure of *S. cerevisiae* α-glucosidase has not been available so far and therefore, we performed docking studies with the homology model, built and described previously [37]. It was characterized by high quality. The active site contained important, from the viewpoint of hydrolysis, amino acids: two histidines (His111, His348), two aspartates (Asp214, Asp349) and one glutamate (Glu276).

It was noted that all compounds presented one main, shared binding mode but the docking runs were really converged only for the active derivatives (with determined IC_{50} values). Moreover, the hydrophilic substituents such as hydroxyl groups were responsible for the interactions, essential for the activity. The core of molecules was engaged in some interactions but they were not enough to provide the high inhibition of enzyme.

The imidazole ring created π – cation interaction with Arg439, and its NH fragment was involved in hydrogen bond with Asp349. The phenyl group in position 5 of imidazole formed other π – cation interaction with Arg312, and phenyl in position 4 weak CH–π interaction with Phe158. The third phenyl moiety in position 2 (derivatives **3a**–**3h**) created π–π stacking interaction with Phe177. In case of compounds **3i** and **3j**, replacement of that phenyl group by alkyl chain was responsible for very low activity due to lack of π–π interaction. Introduction of hydrophilic substituents with H-bond donating properties in the third phenyl ring led to extra interactions and increase of the activity. The hydroxyl group in *ortho* position (compound **3c**, Fig. 3) was both donor (OH → $^{-}$OOC of Asp68) and acceptor (HO ← $H_2N{-}C(=NH_2^{+}){-}NH_2$ of Arg439) of hydrogen bonds. Movement of hydroxyl substituent into *para* position (compound **3f**) caused small decrease of potency

Table 1
Percent yield, α-glucosidase inhibition activity and IC_{50} values (mean ± SEM, $n = 3$) of 2,4,5-trisubstituted imidazoles (ND, not determined).

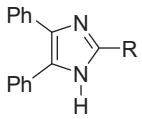

Entry	Products	*R*	Yield (%)	% Inhibition (0.5 mM)	IC_{50} (μM)
1.	3**a**	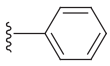	78	28.75 ± 2.18	ND
2.	3**b**	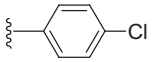	76	51.53 ± 2.37	458.32 ± 1.14
3	3**c**	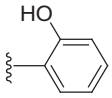	70	97.63 ± 1.29	74.32 ± 0.52
4.	3**d**	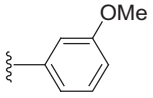	62	89.23 ± 2.45	359.42 ± 1.12
5.	3**e**	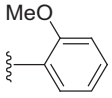	76	11.09 ± 1.41	ND
6.	3**f**	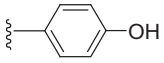	85	97.18 ± 1.45	97.12 ± 0.71
7.	3**g**	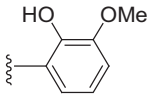	71	96.63 ± 1.11	106.57 ± 0.86
8.	3**h**	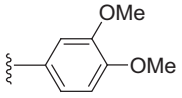	67	20.76 ± 1.16	ND
9.	3**i**	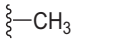	67	8.76 ± 1.76	ND
10.	3**j**	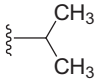	73	17.56 ± 1.85	ND
11.	Acarbose	–	–	92.23 ± 0.14	38.25 ± 0.12

in comparison with *ortho* substituted inhibitor **3c** because OH group formed only one H-bond with Asp214 (OH → $^{-}$OOC of Asp214). Further modifications, including introduction of methoxy substituents decreased the activity in comparison with hydroxy derivatives (**3c**, **3f**) because methoxy groups were only H-bond acceptors (compounds **3e**, **3d**, **3h**), and in case of derivative **3e** (*o*-methoxy analogue of **3a**) additionally led to steric clash. Only compound **3g**, which contained both hydroxyl and methoxyl substituents, displayed similar activity to inhibitor **3f** due to hydrogen bond between hydroxyl group in *ortho* position and Arg439, which

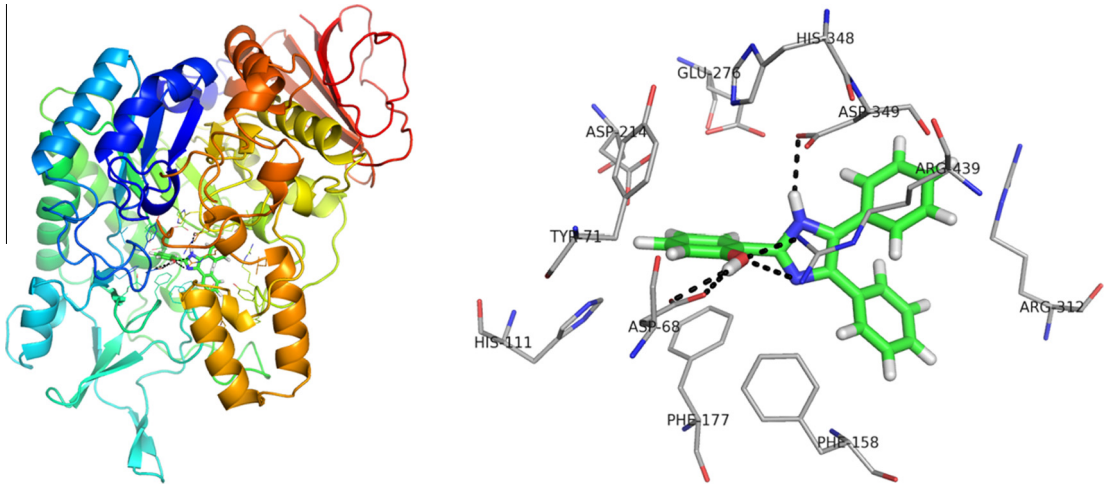

Fig. 3. General view of baker's yeast α-glucosidase with docked compound **3c** (left). Detailed binding mode of inhibitor **3c** (right; black lines represent hydrogen bonds).

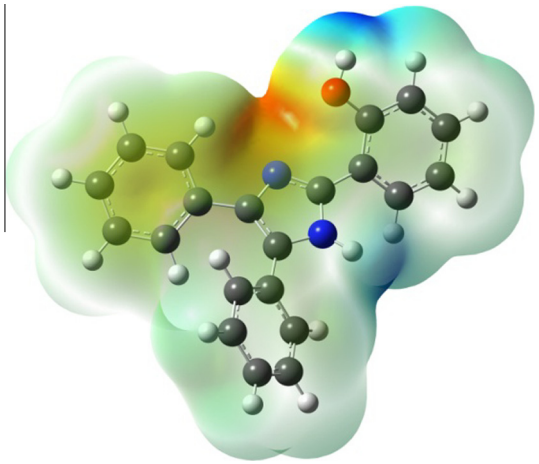

Fig. 4. Molecular electrostatic potential map of **3c** calculated at B3LYP/6-31G(d,p).

decreased undesirable effect of phenyl rotation, caused by presence of —OCH_3. Compound **3b** with chlorine atom was weak inhibitor. Halogen bond between Cl and Asp68 was not enough to increase the activity in a large extent.

It seems that introduction of some extra hydroxyl substituents in phenyl rings could improve the inhibitory potency of novel derivatives.

Comparing scoring function for all derivatives (**3a**–**3j**) with score for acarbose, it was noted that they had been worst assessed than reference inhibitor. It remained in accordance with experimental results and suggested that some further derivatives should be developed.

3. Computational studies

Molecular electrostatic potential (MEP) is associated with the electronic density and it describes the sites for electrophilic and nucleophilic reactions as well as hydrogen bonding interactions [49,50]. Usually, the preferred nucleophilic site is represented by red color and the preferred electrophilic site is represented by blue color. The different values of the electrostatic potential at the surface are represented by different colors. Potential increases in the order red < orange < yellow < green < blue. The color code of the map is in the range between −0.0693 a.u. (deepest red) and 0.0693 a.u. (deepest blue) in the compound, where blue shows the strongest attraction and red shows the strongest repulsion. Regions of negative V(r) is usually associated with the lone pair of electronegative atoms.

From the docking studies, it was revealed that NH fragment of the imidazole and the hydroxy group attached to aromatic ring were responsible for making hydrogen bonds making the molecule more potent. It is further supported by generating molecular electrostatic potential map of the most active molecule **3c** (Fig. 4). The blue regions (NH and OH groups) indicate the most electrophilic sites of the molecule and are involved in hydrogen bonding.

4. Conclusion

In conclusion, 2,4,5-trisubstituted imidazoles were synthesized by employing a new catalyst (NAG) under solvent free reaction conditions. The *in vitro* α-glucosidase inhibitory activity of these compounds revealed that compounds **3c**, **3f** and **3g,** all bearing a hydroxyl group in the 2-phenyl ring, were found to be significantly active. Compound **3c**, being the most active, was subjected to *in silico* molecular docking and computational studies. Finding of these inhibitors may lead to future non-glucosidic based inhibitors.

5. Experimental

5.1. General methods

Infrared spectra were recorded on a photo acoustic mode at the frequency range of 4000–400 cm^{-1} with 256 consecutive scans at a 8 cm^{-1} resolution on a Thermo-Nicolet 6700 P FTIR Spectrometer (USA). ^1H NMR spectra were recorded on a AC-Bruker 300 MHz spectrometer in $CDCl_3$ and DMSO-d_6 containing TMS as internal standard. Splitting patterns were as follows s (singlet), d (doublet), dt (doublet of triplet), dd (double doublets), t (triplet), and m (multiplet). All *J* values are given in Hz and chemical shifts in δ-units. The progress of all reactions was monitored by TLC, which was performed on 2.0 × 5.0 cm aluminum sheets precoated with silica gel $60F_{254}$ to a thickness of 0.25 mm (Merck). The chromatograms were visualized under ultraviolet light (254–366 nm).The melting points were determined on a capillary melting point apparatus and are uncorrected. Mass spectra were recorded on a Varian MAT 312 double focusing spectrometer, connected to an IBM-AT compatible PC computer system. Chemical reagents were purchased from the Merck Chemical Company in high purity. All the materials were of commercial grade reagent.

5.2. General procedure for the synthesis of 2,4,5-trisubstituted imidazoles (*3a*–*3j*)

A mixture of 1 g benzil (1 mmol), 0.733 g ammonium acetate (2 mmol), 0.557 g N-acetyl glycine (1 mmol) and the corresponding aldehyde (1 mmol) was ground in a mortar and pestle while mixed thoroughly. The mixture was then transferred to a 50 mL round bottom flask, equipped with an efficient guard tube and was heated under stirring 150 °C for 2 h. Progress of the reaction was monitored by a TLC. After completion of the reaction, the reaction mixture was diluted with 5% $NaHCO_3$ and extracted with ethyl acetate. The organic layer was separated, dried over Na_2SO_4 and evaporated. The resulting residues were kept overnight at −18 °C to afford solid, which was recrystallized from methanol to obtain pure products **3a**–**3j**. The physical and spectral data of compounds **3a**–**3j** were in complete agreement with previous reports [25,32–35,42].

5.2.1. 2,4,5-Triphenyl-1H-imidazole (*3a*)

White solid, yield: 67%; m.p: 270–272 °C; FT-IR (υ_{max}, cm^{-1}): 3230 (N—H), 3058 (Ar C—H), 2851 (Alkyl C—H), 1678 (C=N), 1600 (C=C); ^1H NMR (400 MHz, DMSO-*d6*): δ 12.61 (s, 1H, NH), 8.16 (d, 2H, Ar-H), 7.69–7.09 (m, 13H, Ar-H); MS (EI) *m/z* 296 (M^+).

5.2.2. 2-(4-Chlorophenyl)-4,5-diphenyl-1H-imidazole (*3b*)

Pale yellow solid, yield: 67%; m.p: 260–265 °C; FT-IR (υ_{max}, cm^{-1}): 3227 (N—H), 3059 (Ar C—H), 2839 (Alkyl C—H), 1678 (C=N), 1599 (C=C); ^1H NMR (400 MHz, DMSO-*d6*): δ 12·75 (s, 1H, NH), 7.96 (d, 2H, Ar-H), 7.43–7.22 (m, 12H, Ar-H); MS (EI) *m/z* 330 (M^+).

5.2.3. 2-(4,5-Diphenyl-1H-imidazol-2-yl)phenol (*3c*)

Pale yellow solid, yield: 67%; m.p: 200–202 °C; FT-IR (υ_{max}, cm^{-1}): 3228 (N—H), 3061 (Ar C—H), 2841 (Alkyl C—H), 1677 (C=N), 1594 (C=C); ^1H NMR (400 MHz, DMSO-*d6*): δ 13.01 (s, 1H, NH), 9.61 (s, 1H, O—H), 8.32 (d, 1H, Ar-H), 7.60–6.73 (m, 13H, Ar-H); MS (EI) *m/z* 312 (M^+).

5.2.4. 2-(3-Methoxyphenyl)-4,5-diphenyl-1H-imidazole (*3d*)

White solid, yield: 67%; m.p: 260–262 °C; FT-IR (υ_{max}, cm^{-1}): 3058 (N—H), 3055 (Ar C—H), 2845 (Alkyl C—H), 1676 (C=N),

1589 (C=C); ^{1}H NMR (400 MHz, DMSO-*d6*): δ 12.97 (s, 1H, NH), 7.66–6.90 (m, 14H, Ar-H), 3.88 (s, 3H, OCH_3); MS (EI) *m/z* 326 (M^+).

*5.2.5. 2-(2-Methoxyphenyl)-4,5-diphenyl-1H-imidazole (**3e**)*

Pale yellow solid, yield: 67%; m.p: 210–212 °C; FT-IR (υ_{max}, cm^{-1}): 3232 (N—H), 3060 (Ar C—H), 2839 (Alkyl C—H), 1677 (C=N), 1585 (C=C); ^{1}H NMR (400 MHz, DMSO-*d6*): δ 12.91 (s, 1H, NH), 8.53 (d, 1H, Ar-H), 7.59–7.02 (m, 13H, Ar-H), 4.04 (s, 3H, OCH_3); MS (EI) *m/z* 326 (M^+).

*5.2.6. 4-(4,5-Diphenyl-1H-imidazol-2-yl)phenol (**3f**)*

Yellow solid yield: 67%; m.p: 235–237 °C; FT-IR (υ_{max}, cm^{-1}): 3227 (N—H), 3055 (Ar C—H), 2844 (Alkyl C—H), 1679 (C=N), 1594 (C=C); ^{1}H NMR (400 MHz, DMSO-*d6*): δ 12.35 (s, 1H, NH), 9.54 (s, 1H, O—H), 7.89 (d, 2H, Ar-H), 7.53–7.21 (m, 10H, Ar-H), 6.87 (d, 2H, Ar-H); MS (EI) *m/z* 312 (M^+).

*5.2.7. 2-(4,5-Diphenyl-1H-imidazol-2-yl)-6-methoxyphenol (**3g**)*

Pale yellow solid, yield: 67%; m.p: 170–172 °C; FT-IR (υ_{max}, cm^{-1}): 3236 (N—H), 3063 (Ar C—H), 2842 (Alkyl C—H), 1690 (C=N), 1589 (C=C); ^{1}H NMR (400 MHz, DMSO-*d6*): δ 12.95 (s, 1H, NH), 9.61 (s, 1H, O—H), 8.32 (d, 1H, Ar-H), 7.60–6.73 (m, 13H, Ar-H), 3.89 (s, 3H, OCH_3); MS (EI) *m/z* 342 (M^+).

*5.2.8. 2-(3,4-Dimethoxyphenyl)-4,5-diphenyl-1H-imidazole (**3h**)*

Pale yellow solid, yield: 67%; m.p: 213–215 °C; FT-IR (υ_{max}, cm^{-1}): 3231 (N—H), 3066 (Ar C—H), 2838 (Alkyl C—H), 1680 (C=N), 1602 (C=C); ^{1}H NMR (400 MHz, DMSO-*d6*): δ 12.93 (s, 1H, NH), 7.73 (d, 1H, Ar-H), 7.26–6.86 (m, 12H, Ar-H), 3.94 (s, 3H, OCH_3); MS (EI) *m/z* 356 (M^+).

*5.2.9. 2-Methyl-4,5-diphenyl-1H-imidazole (**3i**)*

Pale yellow solid, yield: 67%; m.p: 240–242 °C; FT-IR (υ_{max}, cm^{-1}): 3215 (N—H), 3067 (Ar C—H), 2848 (Alkyl C—H), 1681 (C=N), 1561 (C=C); ^{1}H NMR (400 MHz, DMSO-*d6*): δ 13.11 (s, 1H, NH), 7.55–7.34 (m, 10H, Ar-H), 2.56 (s, 3H, CH_3); MS (EI) *m/z* 234 (M^+).

*5.2.10. 4,5-Diphenyl-2-(propan-2-yl)-1H-imidazole (**3j**)*

Pale yellow solid, yield: 67%; m.p: 230–232 °C; FT-IR (υ_{max}, cm^{-1}): 3230 (N—H), 3063 (Ar C—H), 2839 (Alkyl C—H), 1686 (C=N), 1584 (C=C); ^{1}H NMR (400 MHz, DMSO-*d6*): δ 12.93 (s, 1H, NH), 7.66–7.26 (m, 10H, Ar-H), 3.18 (d, 1H, C—H), 1.25 (d, 6H, CH_3); MS (EI) *m/z* 262 (M^+).

5.3. α-Glucosidase inhibition assay

A slightly modified method of Pierre et al. (1978) was adopted for α-glucosidase inhibition assay. A 100 μL assay mixture containing 70 μL phosphate buffer saline (50 mM at pH 6.8), 10 μL corresponding test compounds dissolved in methanol/DMSO (0.5 mM) and 10 μL (0.057 units) α-glucosidase enzyme were mixed, pre incubated for 10 min at 37 °C and the absorbance was recorded at 400 nm using Synergy HT BioTek (USA) 96-well plate reader. The reaction was initiated by the addition of 10 μL p-nitrophenyl-α-D-glucopyranoside (substrate, 0.5 mM/well, code No. N1377 from Sigma Inc.).

The change in absorbance of p-nitrophenol formed was recorded at 400 nm after 30 min of incubation at 37 °C. Both positive and negative controls were run. Acarbose was used as positive control at 0.5 mM concentration. All experiments were carried out in triplicate and results are mean ± SEM. For the determination of IC_{50} values, suitable dilutions of active compounds were carried out for the assay. Data was computed for the determination of IC_{50} values using EZ-Fit Enzyme kinetics software (Perrella Scientific Inc. Amherst, USA).

The percent inhibition was calculated by the following equation;

$$\text{Inhibition}(\%) = 100 - (\text{Abs. of test}/\text{Abs. of control}) \times 100$$

α-Glucosidase (Cat No. 5003-1KU Type I) from *Saccharomyces cerevisiae* has been used in the assay because of the structural and functional similarities between the yeast (eukaryote) and mammalian enzyme (eukaryote).

5.4. Molecular modeling studies

The three-dimensional structures of the compounds were built with Corina on-line tool [52] and subsequently prepared in Sybyl X-1.1 [53]. All atom and bond types, protonation states were checked and later Gasteiger-Marsili charges were added. The homology model of the baker's yeast α-glucosidase, developed in the previously described way [37], was used for dockings with Gold 5.1 software [54]. All histidine residues were set as Nε (HSE) tautomers and ligand (glucose which was taken into account during model building) was removed. The active site was defined as all amino acid residues within 15 Å from that glucose molecule. Dockings were performed using genetic algorithm with default settings. GoldScore function and analysis of binding mode were applied to find final ligand poses. The docking method was previously validated, based on reference inhibitor – acarbose [37]. Results were viewed in PyMOL 0.99rc2 [55].

5.5. Computational studies

The processes based on the "recognition" of one molecule by another, as in drug-receptor, and enzyme substrate interactions are related to electrostatic potential V(r), because the two species come close to each other through their potentials. For the systems studied the MEP values were calculated as described previously, using the following equation [51]:

$$V(r) = \sum \frac{Z_A}{|R_A - r|} - \int \frac{\rho(r')}{|r' - r|} dr'$$

where the summation runs over all the nuclei A in the molecule and polarization and reorganization effects are ignored. Z_A is the charge of the nucleus A, located at R_A and $\rho(r')$ is the electron density function of the molecule. All calculations were performed with Gaussian 09 [56]. The geometries of the structures were optimized at hybrid B3LYP [57,58] method with 6-31G (d,p) basis set.

Conflict of interest

Authors declare no conflict of interest.

Acknowledgments

Molecular modeling studies were financially supported by Polish National Center of Science, Postdoctoral Research Grant No. DEC-2012/04/S/NZ2/00116.

References

[1] Y.-G. Chen, P. Li, P. Li, R. Yan, X.-Q. Zhang, Y. Wang, et al., Molecules 18 (2013) 4221–4232.
[2] G. Danaei, M. Finucane, Y. Lu, G. Singh, M. Cowan, C. Paciorek, et al., Lancet 378 (2011) 31–40.
[3] N. Asano, Glycobiology 13 (2003) 93R–104R.
[4] R.R. Holman, C.A. Cull, R.C. Turner, Diabetes Care 22 (1999) 960–964.
[5] M.J. Humphries, K. Matsumoto, S.L. White, K. Olden, Cancer Res. 46 (1986) 5215–5222.
[6] H. Park, K.Y. Hwang, K.H. Oh, Y.H. Kim, J.Y. Lee, K. Kim, Bioorg. Med. Chem. 16 (2008) 284–292.

[7] S.J. Storr, L. Royle, C.J. Chapman, U.M.A. Hamid, J.F. Robertson, A. Murray, et al., Glycobiology 18 (2008) 456–462.
[8] D.P. Gamblin, E.M. Scanlan, B.G. Davis, Chem. Rev. 109 (2008) 131–163.
[9] H. Park, K.Y. Hwang, Y.H. Kim, K.H. Oh, J.Y. Lee, K. Kim, Bioorg. Med. Chem. Lett. 18 (2008) 3711–3715.
[10] A.J. Rawlings, H. Lomas, A.W. Pilling, M.J.R. Lee, D.S. Alonzi, J. Rountree, et al., Chem. Biol. Chem. 10 (2009) 1101–1105.
[11] D. Schmidt, W. Frommer, B. Junge, L. Muller, W. Wingender, E. Truscheit, et al., Naturwissenschaften 64 (1977) 535–536.
[12] L.J. Scott, C.M. Spencer Miglitol, Drugs 59 (2000) 521–549.
[13] T. Matsuo, H. Odaka, H. Ikeda, Am. J. Clin. Nutr. 55 (1992). 314S-7S.
[14] N. Asano, K. Oseki, E. Tomioka, H. Kizu, K. Matsui, Carbohydr. Res. 259 (1994) 243–255.
[15] P. Hollander, Drugs 44 (1992) 47–53.
[16] S. Adisakwattana, K. Sookkongwaree, S. Roengsumran, A. Petsom, N. Ngamrojnavanich, W. Chavasiri, et al., Bioorg. Med. Chem. Lett. 14 (2004) 2893–2896.
[17] S. Sou, S. Mayumi, H. Takahashi, R. Yamasaki, S. Kadoya, M. Sodeoka, et al., Bioorg. Med. Chem. Lett. 10 (2000) 1081–1084.
[18] J. Lee, J. Laydon, P. McDonnell, T. Gallagher, S. Kumar, D. Green, S.W. Land vatter, J.E. Strickler, M.M. McLaughlin, I.R. Siemens, S.M. Fisher, G.P. Livi, J.R. White, J.L. Adams, P.R. Young, Nature 372 (1994) 739–746.
[19] A.K. Takle, M.J. Brown, S. Davies, D.K. Dean, G. Francis, A. Gaiba, et al., Bioorg. Med. Chem. Lett. 16 (2006) 378–381.
[20] I.K. Khanna, R.M. Weier, Y. Yu, X.D. Xu, F.J. Koszyk, P.W. Collins, et al., J. Med. Chem. 40 (1997) 1634–1647.
[21] J.H. Lange, H.H. van Stuivenberg, H.K. Coolen, T.J. Adolfs, A.C. McCreary, H.G. Keizer, et al., J. Med. Chem. 48 (2005) 1823–1838.
[22] T.F. Gallagher, S.M. Fier-Thompson, R.S. Garigipati, M.E. Sorenson, J.M. Smietana, D. Lee, et al., Bioorg. Med. Chem. Lett. 5 (1995) 1171–1176.
[23] K.P. Chooi, S.R. Galan, R. Raj, J. McCullagh, S. Mohammed, L.H. Jones, et al., J. Am. Chem. Soc. 136 (2014) 1698–1701.
[24] S. Samai, G.C. Nandi, P. Singh, M. Singh, Tetrahedron 65 (2009) 10155–10161.
[25] A. Teimouri, A.N. Chermahini, J. Mol. Catal. A: Chem. 346 (2011) 39–45.
[26] H. Zang, Q. Su, Y. Mo, B.-W. Cheng, S. Jun, Ultrason. Sonochem. 17 (2010) 749–751.
[27] A.R. Khosropour, Ultrason. Sonochem. 15 (2008) 659–664.
[28] M. Xia, Y-d. Lu, J. Mol. Catal. A: Chem. 265 (2007) 205–208.
[29] S.E. Wolkenberg, D.D. Wisnoski, W.H. Leister, Y. Wang, Z. Zhao, C.W. Lindsley, Org. Lett. 6 (2004) 1453–1456.
[30] M.V. Chary, N.C. Keerthysri, S.V. Vupallapati, N. Lingaiah, S. Kantevari, Catal. Commun. 9 (2008) 2013–2017.
[31] L. Wang, C. Cai, Monatshefte für Chemie-Chemical Monthly 140 (2009) 541–546.
[32] M. Saffari Jourshari, M. Mamaghani, F. Shirini, K. Tabatabaeian, M. Rassa, H. Langari, Chin. Chem. Lett. 24 (2013) 993–996.
[33] B.F. Mirjalili, A. Bamoniri, M.A. Mirhoseini, Scientia Iranica, Trans. C: Chem. Chem. Eng. 20 (2013) 587–591.
[34] H. Roy, M. Rahman, P. Pramanick, Indian J. Chem. Section B-Org. Chem. Incl. Med. Chem. 52 (2013) 153–159.
[35] D.I. MaGee, M. Bahramnejad, M. Dabiri, Tetrahedron Lett. 54 (2013) 2591–2594.
[36] R.S. Joshi, P.G. Mandhane, M.U. Shaikh, R.P. Kale, C.H. Gill, Chin. Chem. Lett. 21 (2010) 429–432.
[37] M. Yar, M. Bajda, L. Shahzadi, S.A. Shahzad, M. Ahmed, M. Ashraf, U. Alam, I.U. Khan, A.F. Khan, Bioorg. Chem. 54 (2014) 96–104.
[38] S.A. Shahzad, M. Yar, M. Bajda, B. Jadoon, Z.A. Khan, S.A.R. Naqvi, A.J. Shaikh, K. Hayat, A. Mahmood, N. Mahmood, S. Filipek, Bioorg. Med. Chem. 22 (2014) 1008–1015.
[39] M. Yar, M. Bajda, R.A. Mehmood, L.R. Sidra, N. Ullah, L. Shahzadi, M. Ashraf, T. Ismail, S.A. Shahzad, Z.A. Khan, S.A.R. Naqvi, N. Mahmood, Lett. Drug Des. Discov. 11 (2014) 331–338.
[40] M. Yar, L.R. Sidra, E. Pontiki, N. Mushtaq, M. Ashraf, R. Nasar, I.U. Khan, N. Mahmood, S.A.R. Naqvi, Z.A. Khan, S.A. Shahzad, J. Iran. Chem. Soc. 11 (2014) 369–378.
[41] S. Riaz, I.U. Khan, M. Yar, M. Ashraf, T.U. Rehman, A. Shaukat, S.B. Jamal, V.C.M. Duarte, M.J. Alves, Bioorg. Chem. 57 (2014) 148–154.
[42] K. Ramesh, S.N. Murthy, K. Karnakar, Y. Nageswar, K. Vijayalakhshmi, B.L. Prabhavathi Devi, et al., Tetrahedron Lett. 53 (2012) 1126–1129.
[43] M. Balba, N.A. El-Hady, N. Taha, N. Rezki, E.S.H. El Ashry, Eur. J. Med. Chem. 46 (2011) 2596–2601.
[44] R. Schowen, J. Liebman, A. Greenberg, Mechanistic Principles of Enzyme Activity, VCH, New York, 1988. 119.
[45] M.L. Sinnott, Chem. Rev. 90 (1990) 1171–1202.
[46] A.J. Kirby, Crit. Rev. Biochem. Mol. Biol. 22 (1987) 283–315.
[47] M.P. Dale, W.P. Kopfler, I. Chait, L.D. Byers, Biochemistry 25 (1986) 2522–2529.
[48] R. Field, A.H. Haines, E. Chrystal, M.C. Luszniak, Biochem. J. 274 (1991) 885–889.
[49] F.J. Luque, J.M. López, M. Orozco. Perspective on "electrostatic interactions of a solute with a continuum. A direct utilization of ab initio molecular potentials for the prevision of solvent effects". Theoretical Chemistry Accounts: Springer; 2001. p. 343–5.
[50] E. Scrocco, J. Tomasi, Adv. Quant. Chem. 11 (1978) 115–193.
[51] P. Politzer, P.R. Laurence, K. Jayasuriya, Environ. Health Perspect. 61 (1985) 191.
[52] Corina on-line, <http://www.molecular-networks.com/online_demos/corina_demo>.
[53] Sybyl-X 1.1, Tripos, St. Louis, MO, USA, 2010.
[54] Gold 5.1, The Cambridge Crystallographic Data Centre, Cambridge, UK, 2011.
[55] PyMOL 0.99rc6, DeLano Scientific LLC: Palo Alto, CA, USA, 2006.
[56] M. Frisch, G. Trucks, H. Schlegel, G. Scuseria, M. Robb, J. Cheeseman, et al. Gaussian 09, Rev. C. 01, Gaussian. Inc., Wallingford CT, 2009.
[57] A.D. Becke, J. Chem. Phys. 98 (1993) 5648–5652.
[58] C. Lee, W. Yang, R.G. Parr, Phys. Rev. B 37 (1988) 785.